USING A TCSC FOR LINE POWER SCHEDULING AND SYSTEM OSCILLATION DAMPING – SMALL SIGNAL AND TRANSIENT STABILITY STUDIES

Nelson Martins, Fellow — Herminio J.C.P. Pinto, Member
CEPEL
P.O. Box 68007
21944-970 – Rio de Janeiro – RJ – BRAZIL
nelson@cepel.br hppinto@cepel.br

John J. Paserba, Senior Member
Mitsubishi Electric Power Products, Inc.
512 Keystone Drive
Warrendale, PA 15086 USA
john.paserba@meppi.mea.com

Abstract – This paper describes, in a tutorial manner, TCSC control aspects illustrated through simulation results on a small power system model. The analysis and design of the TCSC controls, to schedule line power and damp system oscillations, are based on modal analysis, and time and frequency response techniques. Transient stability results are included, to validate and refine the TCSC controller design and protection logic under large disturbances.

Keywords – FACTS Controllers, Eigenanalysis, Controller Design, System Oscillations, Power Flow, Transient Stability

1. INTRODUCTION

The potential benefits of Flexible AC Transmission Systems (FACTS) are now widely recognized by the power system engineering community [1,2]. Two Thyristor Controlled Series Compensation devices (TCSC) [3,4], along with a Thyristor Switched Series Capacitor (TSSC), have been in operation for some time in North America [5]. Two other TCSCs were commissioned in early 1999 in South America [6]. The short-term need to assess the impact of FACTS technology has led to R&D efforts on modeling, methodologies and software for static and dynamic analyses, and control strategies. Dynamic studies must contemplate both low and high frequency phenomena, calling for the use of different computer tools.

This paper deals with TCSC control aspects under both small signal and large disturbance conditions. A tutorial exercise on TCSC oscillation damping control and line power scheduling strategies is presented using a small power system model. An alternative control structure is proposed for the practical implementation of the "constant angle" strategy [7]. This strategy allows the rerouting of incremental power transfers in interconnected power systems. Eigenvalue, frequency domain, step response and transient stability results are provided. The data on the example power system utilized are provided in the Appendix so the results may be reproduced or expanded upon by others.

2. TCSC CONTROLS AND POWER SYSTEM MODEL DESCRIPTION

The example system model (see Fig. 1 and Appendix) comprises a 5-unit hydro power plant connected to an infinite bus through a step-up transformer followed by two transmission circuits. The two operating points considered correspond to generation levels of 1000 MW or 800 MW in the case of a line outage.

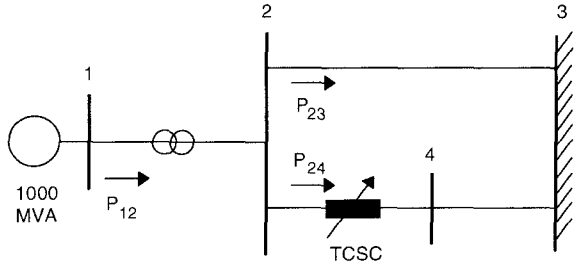

Fig. 1. Small Power System with TCSC.

The generator has a 5th order model with data described in the Appendix. The automatic voltage regulator is represented by a first-order transfer function, also given in the Appendix. The TCSC device is located in line 2-4.

2.1 TCSC Model and Control System Diagram

Fig. 2 shows the control system diagram of a TCSC connected to a transmission line, considering also the dynamics of the linearized power system model. The blocks PI(s) and POD(s) denote the transfer functions of the TCSC line power scheduling controller and Power Oscillation Damping (POD) controller, respectively. The blocks $F_1(s)$ and $F_2(s)$ relate the TCSC output (variable line series susceptance, $B_{2\text{-}4}$) to the controlled system variable (x_{cont}) and the input variable to the POD controller, (x_{inp}). Functions $F_1(s)$ and $F_2(s)$ have the same order as the number of system state variables. The symbol x_{ref} denotes the TCSC reference or setpoint, whose value in steady-state is equal to x_{cont} due to the PI controller action.

The TCSC model consists of current injections at buses 2 and 4, which are assumed to be the device terminals. The initial value for its susceptance ($B_{2\text{-}4}^0$) is the line 2-4 series susceptance, which is directly modeled into the power flow equations. The TCSC variable susceptance ($B_{2\text{-}4}$) is given, at any instant, by the summation of two susceptances: B_{PI} (the PI-controller output) and B_{POD} (the POD controller output). The TCSC thyristor firing and other delays are usually represented by a single lag of about 15ms, but were not modeled here for simplicity and because they do not significantly impact the electromechanical stability phenomena [3,8].

A more detailed block diagram of the TCSC Proportional-Integral (PI) and POD controller is given in Fig. 3. The PI control action is quite slow in practice, since the line power scheduling is meant to be done over a period of 30 s. The parameters for the PI controller are given in Fig. 3. The parameters of the POD controller differ according to its input variable (x_{inp}), which could be local bus frequency, line current or power magnitudes, among other possibilities. A typical POD controller structure is depicted in Fig. 3. Note that, while the PI controller is designed to be a slow-acting control, the POD controller provides damping to fairly fast oscillations (0.2 to 2 Hz).

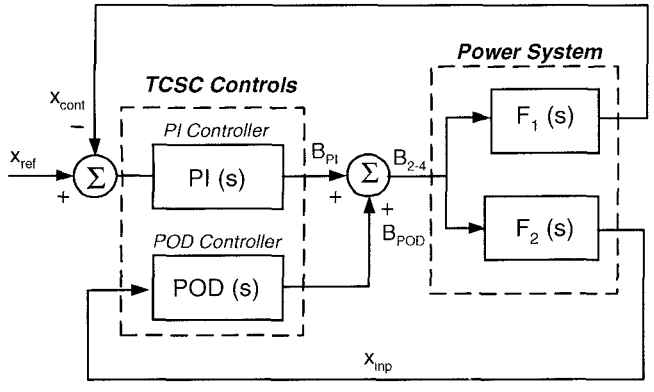

Fig 2. TCSC Control System Diagram.

Note: *The symbol x, (e.g., x_{ref} or x_{inp}) is used here to denote a generic system variable and does not necessarily refer to line reactance.*

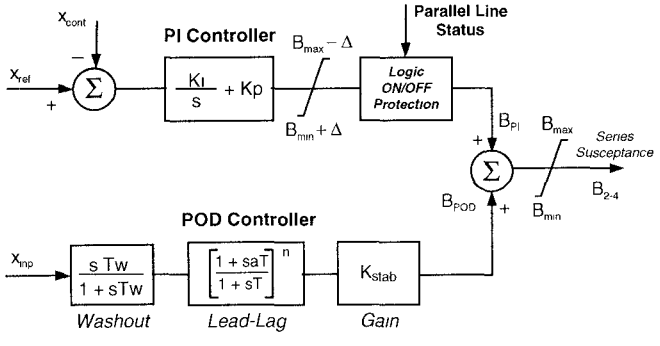

K_I = 5, K_p = 0 5 in all cases B_{max} = 5

$x_{cont} = P_{2\text{-}4}$ for Constant Line Power Strategy B_{min} = 2 5

$x_{cont} = P_{2\text{-}4} + P_{2\text{-}1}$ for Constant Angle Strategy Δ = 0.1

Fig 3. TCSC Controls.

The purpose of the protection logic depicted in Fig. 3 is described in Section 4.

2.2 TCSC Line Power Scheduling Strategies

Two strategies for scheduling the power flow of line 2-4 through the TCSC device were modeled by changing appropriately the x_{cont} signal depicted in Figs. 2 and 3. One strategy keeps the power flow in line 2-4 at a specified value ($x_{cont} = P_{24}$; $x_{ref} = P_{24}^0$) and will here be referred to as "constant line power" strategy. The other strategy makes line 2-4 absorb any changes in generated power ($x_{cont} = P_{24} + P_{21}$; $x_{ref} = P_{24}^0 + P_{21}^0$). The latter is known as the "constant-angle" strategy [7] since it keeps the steady-state flows in parallel fixed impedance paths at constant level.

The "constant angle" control structure proposed in this paper would require the telecommunication of the signal ΔP_{21}, in case it were remote. Using remote signals to implement this control strategy has an impact on costs, but not on its reliability due to the slow speed requirements of the line power scheduling process.

3. SMALL SIGNAL STABILITY AND CONTROL DESIGN RESULTS

The system condition analyzed has a power transfer of 1000 MW, which is a transfer level where oscillation damping has long become a critical issue. Table I displays the system eigenvalues for four different configurations of TCSC controls. Case A corresponds to the system with the TCSC operating at constant reactance mode. Note that in this operating mode, the TCSC controls depicted in Fig. 3 do not exist. The system has six states and shows oscillatory instability ($\lambda = +0.305 \pm j\,6.126$) due to lack of generator damping torque. Case B incorporates a Power Oscillation Damping (POD) controller, which stabilizes the system. The POD controller design is described in the sequel. Case C considers, in addition to the POD controller, the presence of a "constant line power" controller. Case D considers, instead, the presence of the "constant angle" controller, which makes line 2-4 absorb all the power flow changes in line 1-2.

Note from Table I that the electromechanical mode has approximately the same frequency ($\omega \approx 5.8$ rad/s) and damping in cases B, C and D, showing that the slowly acting line power scheduling control of the TCSC does not impact the generator synchronizing and damping torques.

Table I. Eigenvalues for Cases A, B, C and D

Four Configurations of TCSC Controls	
A **TCSC at Constant Reactance Mode**	**B** **With POD Controller**
-17.907	-17 932
-7.841 ± j 5.528	-7.718 ± j5.416
-6.968	-7.665
+0.305 ± j 6.126	-0.890 ± j5 822
	-0 340
C **with POD and Constant Line Power Controllers**	**D** **With POD and Constant Angle Controllers**
-17 931	-17 933
-7 673	-7.663
-7.715 ± j5 419	-7 720 ± j5 415
-0.889 ± j5 771	-0.849 ± j5.829
-0.344	-0.344
-0.123	-0 123

3.1 Design of POD Controller

The electromechanical mode ($\lambda = +0.305 \pm j6.126$) is seen to be unstable for Case A, since the high power transfer level

causes the generator excitation system to produce highly negative damping torques.

Stabilization could be most economically obtained by adding a power system stabilizer to the generator excitation system [9], but here only the TCSC controls will be considered. The design of the POD controller used in Case B is described below.

TCSC stabilizer design is here based on Nyquist plots of a chosen Open Loop Transfer Function (OLTF), considering the control diagram of Fig. 2. The OLTF used for the design of stabilizer POD(s) controller is shown below:

$$\frac{x_{inp}(s)}{B_{POD}(s)} = \frac{F_2(s)}{1 + F_1(s) \cdot PI(s)}$$

Closed loop stability for the open-loop unstable system ($\lambda = +0.305 \pm j6.126$) is obtained by ensuring a counter-clockwise encirclement of the -1 point by the Nyquist plot of the OLTF after feedback compensation. The reader is referred to [10,11] for more information regarding the frequency response design methods of this paper.

Generator speed was chosen as the POD controller input signal ($x_{inp} = \omega$). The speed signal can be inferred from bus voltage and line current measurements at the TCSC location [11]. Alternatively, local bus frequency could be used almost to the same effect. The Nyquist plot in Fig. 4 shows the rotor speed signal needs high amplification but no phase compensation. This result is in agreement with current practice: using a proportional gain provides pure damping torque when the device input is rotor speed or frequency bus and its output affects real power [7, 12]. The POD design, as shown in Fig. 5, includes a large gain and a washout block while ensures that the POD controller output returns to zero after transients.

The effectiveness of the POD controller (Fig. 6) is verified from the eigenvalue results of Table I (Cases B, C and D) and the step response plots in Figs. 7, 8 and 9.

Reference [11] presents other design results, when using line transit power as the input signal to the POD controller. It is shown in [11] that a 90° phase-lag compensation is needed when using the line power signal.

3.2 Step Response

Step response results of the linearized system help evaluate the performance of the two line power scheduling strategies. The applied disturbance is a 1% step in the mechanical power of the synchronous generator (ΔP_{mec}). The monitored variables are the active power flow deviations in the lines of the system (ΔP_{12}, ΔP_{23} and ΔP_{24}).

Figs. 7, 8 and 9 show the step responses for Cases B, C and D, whose eigenvalues are displayed in Table I. The eigenvalues associated with the electromechanical oscillation, which are dominant in these responses, are also shown in the captions of these figures. Fig. 7 refers to Case B and shows that, in the absence of a line power controller, the generated power step change ΔP_{12} is equally shared between the two transmission circuits ($0.5\ \Delta P_{12} = \Delta P_{23} = \Delta P_{24}$). Case C results (Fig. 8) show the power flow in line 2-4 returning to its scheduled pre-disturbance value through the PI-controller action. The increased power transfer eventually flows solely through the parallel path (line 2-3).

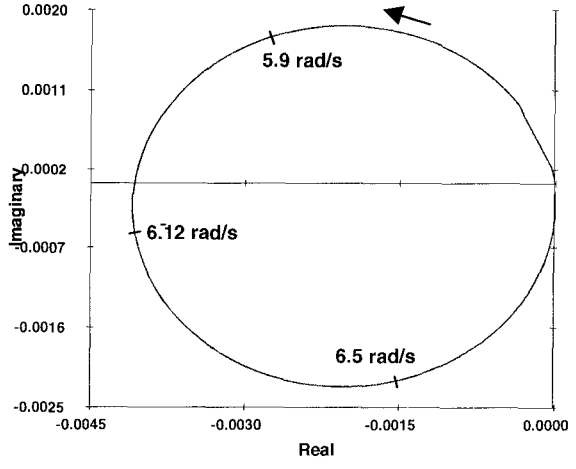

Fig 4. Nyquist Plot of OLTF $\Delta\omega(s)/\Delta B_{POD}(s)$ used for POD Controller Design (Dominant Mode $\lambda = +0.305 \pm j\ 6.126$)

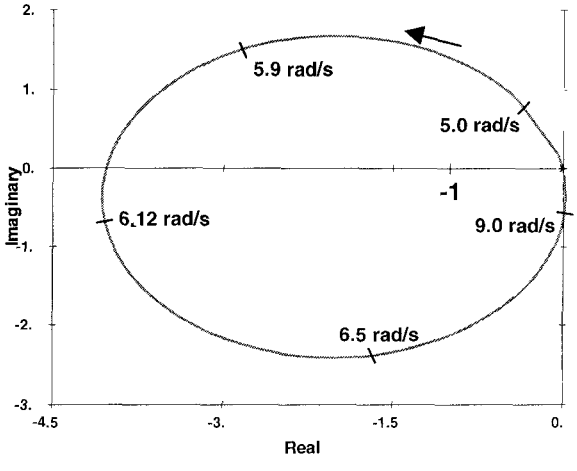

Fig 5. Nyquist Plot of the OLTF $\Delta\omega(s)/\Delta B_{POD}(s)$. POD(s) (Dominant Mode $\lambda = +0.305 \pm j6.126$).

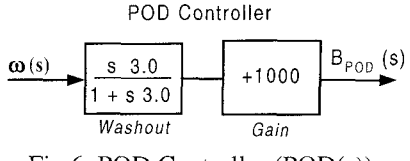

Fig 6. POD Controller (POD(s)).

Case D results (Fig. 9) show the compensated line 2-4 absorbing all of the increased active power generation. The power flow in the parallel path (line 2-3) is seen to settle down at the pre-disturbance value. Note that the electromechanical oscillations ($\omega \approx 5.8$ rad/s) die out after about 5s. The response of the TCSC line power scheduling controller (Figs. 8 and 9) is slow and monotonic, being determined mostly by the real eigenvalue $\lambda = -0.123$.

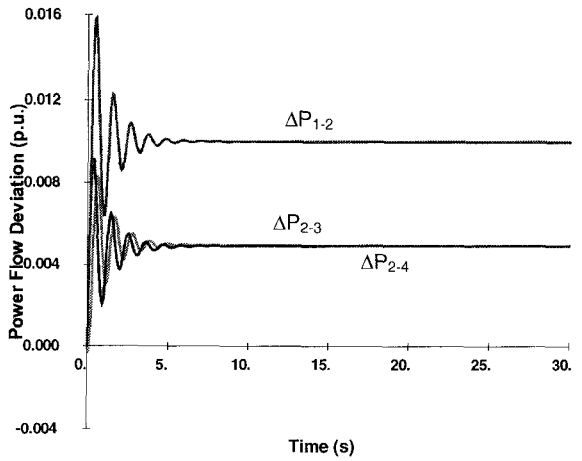

Fig 7. Case B – TCSC with POD Controller (Dominant Mode: $\lambda = -0.890 \pm j5.822$).

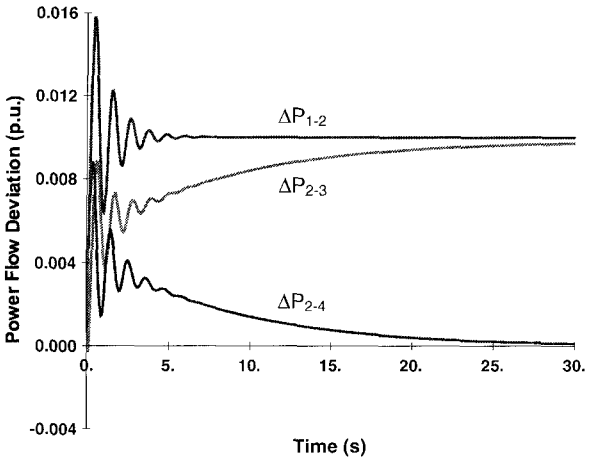

Fig 8. Case C – TCSC with POD and Constant Line Power Controllers (Dominant Modes: $\lambda = -0.889 \pm j5.771$ and $\lambda = -0.123$).

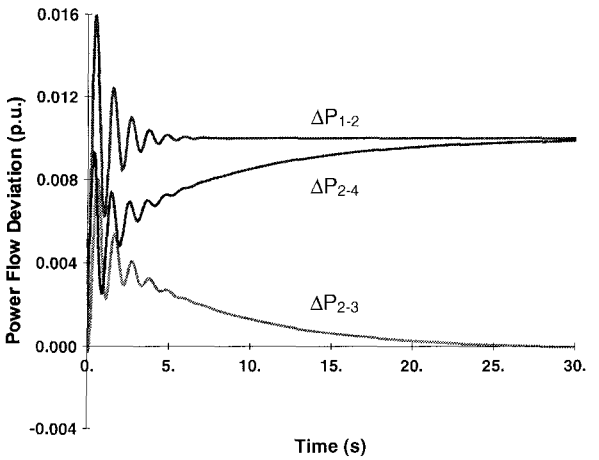

Fig 9. Case D – TCSC with POD and Constant Angle Controllers (Dominant Modes: $\lambda = -0.849 \pm j5.829$ and $\lambda = -0.123$).

The TCSC device was here seen to be very effective for line power scheduling and power system oscillation damping. A controllable device must perform satisfactorily under all system conditions. TCSC controls, for example, must in practice be designed to also avoid potential control problems associated with line outage conditions, as described in Section 4.

4. AVOIDING POTENTIAL PROBLEMS WITH TCSC CONTROLS DURING LINE OUTAGES

Cases E, F and G refer to a line outage condition (line 2-3) with 800 MW generation (4 units connected). Case E refers to the TCSC at constant reactance mode, which again yields an unstable condition ($\lambda = +0.525 \pm j4.927$). In Case F the TCSC has the constant line power controller and the POD controller, as given in Figs. 3 and 6. Note that a zero eigenvalue appears in Case F (see Table II) indicating a total lack of synchronizing torque at steady-state. This serious problem arises because the TCSC PI-controller acts so as to maintain constant power flow in line 2-4 irrespective of angle deviations at its terminals.

Table II. Eigenvalues for Cases E, F and G

Transfer of 800 MW under line outage condition			
E	**TCSC at Constant Reactance Mode**	*F*	**with POD and Constant Line Power Controllers**
	-17.765		-17.872
	-7.711 ± j 6.337		-6.920 ± j6.057
	-6.962		-9.628
	+0.525 ± j 4.927		-2.436 ± j3.534
			-0.366
			0.000
G	**with POD and without Constant Line Power Controllers**		
	-17.878		
	-6.920 ± j6.020		
	-9.620		
	-2.408 ± j3.641		
	-0.366		

This problem did not appear in Case C because line 2-3 was then in-service and provided a free parallel path for synchronizing power exchanges between the generator and the infinite bus.

The linear step response results for Case F are displayed in Fig. 10, showing some serious control problems. The plots of the voltage deviations at buses 2 and 4 are shown in Fig. 10 along with the line 1-2 current deviation. Note that after the step disturbance to the generator mechanical power (ΔP_{mec}), the variables plotted in Fig. 10 either continuously increase or decrease. This is a direct consequence of the fact that the system zero eigenvalue (Case F) became a pole at the origin in all three transfer functions: $\Delta I_{1\text{-}2}(s)/\Delta P_{mec}(s)$, $\Delta V_2(s)/\Delta P_{mec}(s)$ and $\Delta V_4(s)/\Delta P_{mec}(s)$.

The "constant line power" and "constant angle" strategies are meant to be applied to transmission systems having two or

more parallel paths. The unacceptable condition ($\lambda = 0$) observed in the Case F eigensolution and time response results implies that, after any disturbance, the TCSC output would drift to either its maximum or minimum limits. A protection scheme is, therefore, needed to disconnect the TCSC line power scheduling controls during some critical system contingencies. The POD controller must however be left operational during such contingencies to keep the system stable and adequately damped.

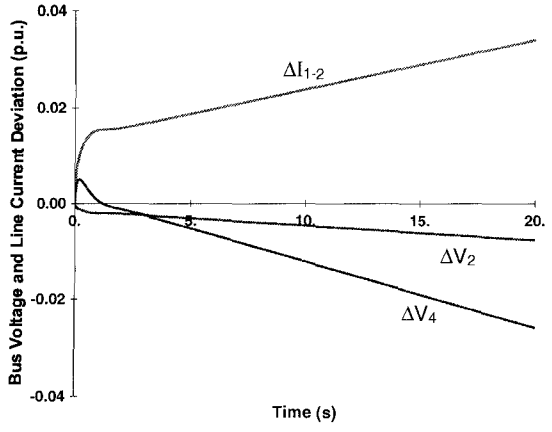

Fig 10. Case F – TCSC with POD and "Constant Line Power" Controller for Line Outage Condition (Dominant Modes: $\lambda = -2.436 \pm j3.534$ and $\lambda = 0$).

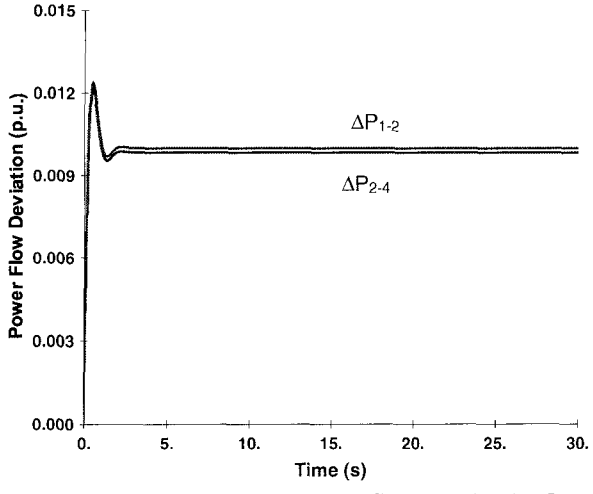

Fig 11. Case G – TCSC with Only POD Controller During Line Outage Condition (Dominant Mode: $\lambda = -2.408 \pm j3.641$)

Case G corresponds to the same line outage condition, but with the PI-controller disconnected while maintaining the POD controller operational. The eigenvalue results are also listed in Table II, showing the zero eigenvalue has disappeared.

The POD(s) transfer function was designed for another line loading condition (Case B) and has excessive gain for this case, yielding very large damping and a significant drop in frequency of the electromechanical mode ($\lambda = -2.408 \pm j3.641$). The step response results for Case G are shown in Fig. 11.

4.1 Transient Stability Results

The large disturbance results studied in this section refer to a fault applied at line 2-3 at t = 0.5s and cleared at t = 0.6s by the tripping of line 2-3. One generator unit is dropped at the time of fault clearing to maintain stability and avoid circuit overloading. Speed-governor dynamics are not modeled. Three simulation cases are shown, the difference among them being only in the level of representation of the TCSC limiters and protection logic.

Fig. 12 refers to the case with POD and "constant line power" controls. Only the output limiter (B_{max}, B_{min}) of the TCSC is active. Note that after fault clearance through line tripping and the dropping of 1 generating unit, the PI-controller input error causes the TCSC output to saturate at B_{max}. Controller saturation (Fig. 12a) prevents POD susceptance modulation in the upper-half cycle. As a result of controller saturation, the system oscillations become poorly damped (Fig. 12b).

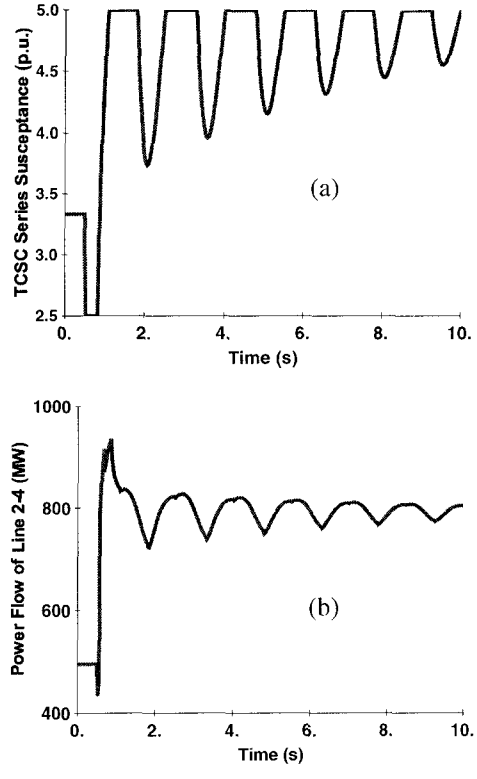

Fig 12. With POD and Constant Line Power Controls. Only the TCSC output limiter (B_{max}, B_{min}) is active.

Fig.13 refers to the case where both limiters shown in Fig. 3 are active: that located in the PI-channel ($B_{max} - \Delta$, $B_{min} + \Delta$) being tighter than the other located at the controller output (B_{max}, B_{min}). In this manner, it is ensured there remains a ±0.1 pu susceptance margin for POD-modulation when the PI-channel saturates. The system response in Fig. 13 is, therefore, seen to eventually become linear and highly damped.

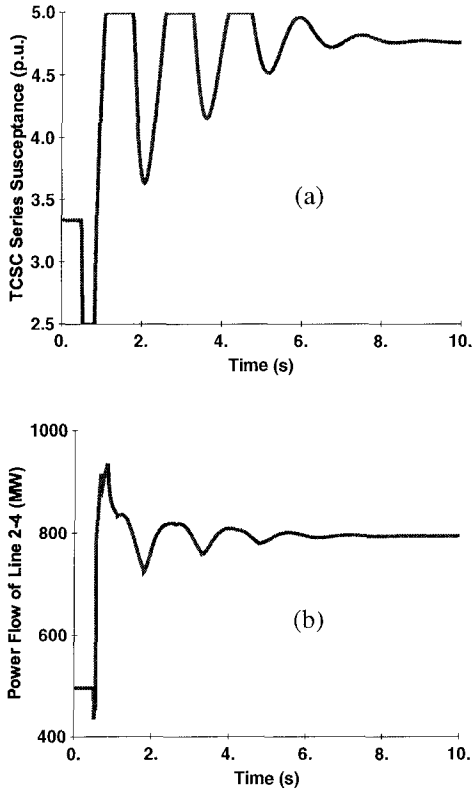

Fig 13. With POD and Constant Line Power Controls. Both TCSC limiters (see Fig. 3) are active.

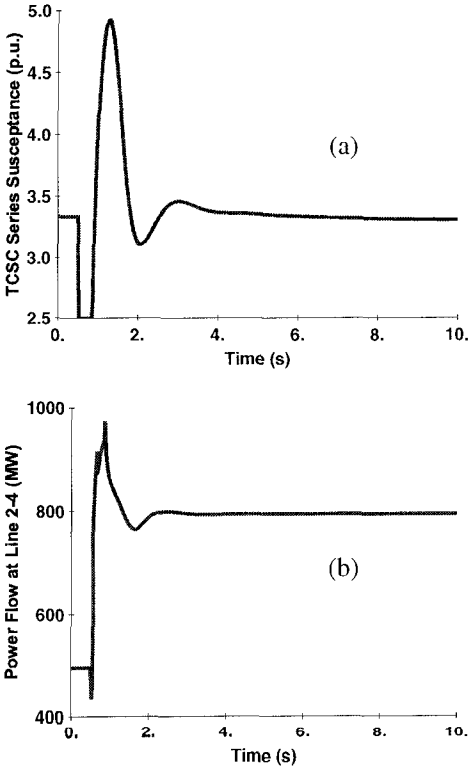

Fig 14. PI-controller channel turned off by protection logic when line 2-3 is tripped.

Fig. 14 refers to the case where the TCSC protection logic (see Fig. 3) is active, switching off the PI-channel when line 2-3 is tripped. Note that, in this case, the TCSC output does not saturate, ensuring adequate POD control and system stabilization.

6. CONCLUSIONS

This paper presented, in a tutorial manner, the application of a TCSC for line power scheduling using both a constant power strategy and a constant angle strategy, and for damping electromechanical oscillations. A small power system model was used, with data provided so that others can reproduce or expand upon the results presented here. Several practical aspects of control design were illustrated including the potential problems of the TCSC control when parallel lines are outaged. The designed TCSC controls and protection logic were seen to be robust, for small as well as large disturbances. The results show the leverage of TCSC for power scheduling and for damping oscillations.

It is known that the effectiveness of the POD controller increases with the active power flowing through the TCSC, being negligible for zero power flow conditions. Practical implementations of POD controllers in TCSCs [6,13] compensate for this changing characteristic, by utilizing a variable gain in the loop, which is reduced as the line power transfer increases. Current digital technology allows easy implementation of this variable gain and other advanced supervisory control functions.

The results of this paper are clear examples of the benefits gained from the use of modal analysis and frequency response tools in addition to the conventional transient stability simulations.

The TCSC power scheduling control responds in the same time frame as secondary voltage controls, AGC and LTCs. Depending on system structure and electrical proximity, these different types of controllers may adversely interact when not properly coordinated.

REFERENCES

[1] IEEE FACTS Working Group 15.05.15 in cooperation with CIGRE, "FACTS Overview," IEEE Special Publication 96-TP-108, 1996.

[2] Task Force on FACTS Applications of the IEEE FACTS Working Group 15.05.15 "FACTS Applications," IEEE Special Publication 96TP116-0, 1996.

[3] R.J. Piwko, C.A. Wegner, B.L. Damsky, B.C. Furumasu, J.D. Eden, "The Slatt Thyristor Controlled Series Capacitor Project-Design, Installation, Commissioning, and System Testing," CIGRE paper 14-104, Paris, 1994.

[4] N. Chistl, R. Hedin, K. Sadek, P. Lutzelberger, P.E. Krause, S.M. McKenna, A.H. Montoya, D. Torgerson, "Advanced Series Compensation (ASC) with Thyristor Controlled Impedance," CIGRE Paper 14/37/38-05, Paris, 1992.

[5] A.J.F. Keri, B.J. Ware R.A. Byron, M. Chamia, P. Halvarsson, L. Angquist, "Improving Transmission System Performance Using Controlled Series Capacitors," CIGRE Paper 14/37/38-07, Paris, 1992.

[6] C. Gama, R.L. Leoni, J.C. Salomão, J.B. Gribel, R. Fraga, M.J.X. Eiras, W. Ping, A. Ricardo, J. Cavalcanti, "Brazilian North-South Interconnection – Application of Thyristor Controlled Series Compensation (TCSC) to Damp Inter-Area Oscillation Mode," SEPOPE Conference, Brazil, May 1998.

[7] E.V. Larsen, C.E.J. Bowler, B. Damsky, S. Nilsson, "Benefits of Thyristor Controlled Series Compensation," CIGRE Paper 14/37/38-04, Paris, 1992.

[8] S. Nyati, C.A. Wegner, R.W. Delmerico, D.H. Baker, R.J. Piwko, A. Edris, "Effectiveness of Thyristor Controlled Series Capacitor in Enhancing Power System Dynamics: An Analog Simulator Study," IEEE Transactions on Power Delivery, April, 1994, pp. 1018-1027.

[9] CIGRE Task Force 38.01.07, "Analysis and Control of Power System Oscillations," CIGRE Technical Brochure No. 111, December 1996

[10] N. Martins and L.T.G. Lima, "Eigenvalue and Frequency Domain Analysis of Small-Signal Electromechanical Stability Problems," IEEE Symposium on Application of Eigenanalysis and Frequency Domain Methods for System Dynamic Performance, Special Publication 90TH0292-3PWR, pp. 17-33, 1990.

[11] N. Martins, H.J.C.P. Pinto and J.J. Paserba, "TCSC Controls for Line Power Scheduling and System Oscillation Damping - Results for a Small Example System", Proceedings of 13th Power System Computation Conference (PSCC), Trondheim, Norway, June 1999.

[12] E.V. Larsen, J.J. Sanchez-Gasca, J.H. Chow, "Concepts for Design of FACTS Controllers to Damp Power Swings," IEEE Transactions on Power Systems, Vol. 10, No. 2, May 1995, pp. 948-956.

[13] C. Gama, "Brazilian North-South Interconnection -Control Application And Operating Experience With A TCSC", *Proceedings of 1999 IEEE PES Summer Meeting*, pp. 1103-1108, Edmont, Canada, July 1999.

APPENDIX

A.1 Example System Data

Frequency: 60 Hz System Base: 1000 MVA

Branch Data for All Cases

Branch		Impedance (%)	
From	To	R	X
1	2	-	10
2	3	6 3	90.
2	4	-	-30.
4	3	6 3	120.

Note that line 2-3 is out-of-service in Cases E, F and G. Line 2-4 the TCSC reactance, which has the same value for the two power flow conditions..

Bus Data for 1000 MW Transfer

Bus	|V| pu	θ degrees	P_{gen} MW	Q_{gen} Mvar
1	1.000	32.8	1000.	219.7
2	0 976	27.0		
3	1.000	0.0	-959.6	356 9
4	1.005	17.9		

Bus Data for 800 MW Transfer Under Line Outage Condition

Bus	|V| pu	θ degrees	P_{gen} MW	Q_{gen} Mvar
1	1 000	51.1	800	315 6
2	0.966	46.5		
3	1.000	0 0	-748.2	424.0
4	1.070	59.8		

Generator Data (5 units of 200 MVA)

H = 5.00	X'_d = 0 30	T'_{do} = 7 50
X_d = 1.00	X''_d = 0.25	T''_{do} = 0.09
X_q = 0 70	X''_q = 0 25	T''_{qo} = 0 20

Reactances are given in per unit; time constants and inertia in seconds. System data is kept as simple as possible. Intermediate voltages in the transmission circuit are low, since no line charging or shunt compensation are modeled.

A.2 Generator Model

The fifth-order model for the synchronous generator is described by the standard equations, with generator saturation effects ignored for the analysis presented in this paper. The remaining system data is given along the text of this paper.

The generator excitation control, for all cases, has the following first order transfer function.

$$AVR(s) = \frac{75}{1 + s\,0.05}$$

BIOGRAPHIES

Nelson Martins B.Sc. (72) Elec. Eng. from Univ. Brasilia, Brazil; M.Sc. (74) and Ph.D. (78) degrees from UMIST, UK. Dr. Martins has worked in CEPEL since 1978. He is the Chairman of CIGRE Task Force 38.02.16 on the Impact of the Interaction Among Power System Controls and has contributed to several IEEE Working Groups.

Herminio J.C.P. Pinto B.Sc. (86), M.Sc. (90) and D.Sc. (98) Elec. Eng. from Federal University of Rio de Janeiro, Brazil. Since 1986 he has been with CEPEL and his current work and interests include power system operation and control and parallel processing.

John J. Paserba BEE (87) from Gannon University, Erie, PA., ME (88) from RPI, Troy, NY. Mr. Paserba worked in GE's Power Systems Energy Consulting Department for over 10 years before joining Mitsubishi Electric in 1998. He is the Chairman of the Power System Stability Subcommittee and he was the Chairman of CIGRE Task Force 38.01.07 on Control of Power System Oscillations, and has contributed to several IEEE Working Groups, Task Forces, and Subcommittees.